

A Novel Type of Stem Cells Double-Positive for SSEA-3 and CD45 in Human Peripheral Blood

Cell Transplantation
Volume 29: 1–16
© The Author(s) 2020
Article reuse guidelines:
sagepub.com/journals-permissions
DOI: 10.1177/0963689720923574
journals.sagepub.com/home/ctj


Tetsuya Sato^{1,2,*}, Shohei Wakao^{1,*}, Yoshihiro Kushida¹,
Kazuki Tatsumi^{1,3}, Masaaki Kitada¹, Takatsugu Abe⁴,
Kuniyasu Niizuma^{4,5}, Teiji Tominaga⁴, Shigeki Kushimoto²,
and Mari Dezawa¹ 

Abstract

Peripheral blood (PB) contains several types of stem/progenitor cells, including hematopoietic stem and endothelial progenitor cells. We identified a population positive for both the pluripotent surface marker SSEA-3 and leukocyte common antigen CD45 that comprises $0.04\% \pm 0.003\%$ of the mononuclear cells in human PB. The average size of the SSEA-3(+)/CD45(+) cells was $10.1 \pm 0.3 \mu\text{m}$ and $\sim 22\%$ were positive for CD105, a mesenchymal marker; $\sim 85\%$ were positive for CD19, a B cell marker; and $\sim 94\%$ were positive for HLA-DR, a major histocompatibility complex class II molecule relevant to antigen presentation. These SSEA-3(+)/CD45(+) cells expressed the pluripotency markers Nanog, Oct3/4, and Sox2, as well as sphingosine-1-phosphate (SIP) receptor 2, and migrated toward SIP, although their adherence and proliferative activities *in vitro* were low. They expressed NeuN at 7 d, Pax7 and desmin at 7 d, and alpha-fetoprotein and cytokeratin-19 at 3 d when supplied to mouse damaged tissues of the brain, skeletal muscle and liver, respectively, suggesting the ability to spontaneously differentiate into triploblastic lineages compatible to the tissue microenvironment. Multilineage-differentiating stress enduring (Muse) cells, identified as SSEA-3(+) in tissues such as the bone marrow and organ connective tissues, express pluripotency markers, migrate to sites of damage via the SIP-SIP receptor 2 system, and differentiate spontaneously into tissue-compatible cells after homing to the damaged tissue where they participate in tissue repair. After the onset of acute myocardial infarction and stroke, patients are reported to have an increase in the number of SSEA-3(+) cells in the PB. The SSEA-3(+)/CD45(+) cells in the PB showed similarity to tissue-Muse cells, although with difference in surface marker expression and cellular properties. Thus, these findings suggest that human PB contains a subset of cells that are distinct from known stem/progenitor cells, and that CD45(+)-mononuclear cells in the PB comprise a novel subpopulation of cells that express pluripotency markers.

Keywords

muse cells, peripheral blood, sphingosine-1-phosphate, SSEA-3, CD45, pluripotency

¹ Department of Stem Cell Biology and Histology, Tohoku University Graduate School of Medicine, Sendai, Japan

² Division of Emergency and Critical Care Medicine, Tohoku University Graduate School of Medicine, Sendai, Japan

³ Regenerative Medicine Division, Life Science Institute, Inc., Tokyo, Japan

⁴ Department of Neurosurgery, Tohoku University Graduate School of Medicine, Sendai, Japan

⁵ Department of Neurosurgical Engineering and Translational Neuroscience, Graduate School of Biomedical Engineering, Tohoku University, Sendai, Miyagi, Japan

* Both the authors contributed equally to this article

Submitted: December 23, 2019. Revised: April 1, 2020. Accepted: April 9, 2020.

Corresponding Authors:

Tetsuya Sato, Division of Emergency and Critical Care Medicine, Tohoku University Graduate School of Medicine, 2-1, Seiryomachi, Aoba-ku, 980-8575 Sendai, Japan.

Shohei Wakao and Mari Dezawa, Department of Stem Cell Biology and Histology, Tohoku University Graduate School of Medicine, 2-1, Seiryomachi, Aoba-ku, 980-8575 Sendai, Japan.

Emails: t23jor@med.tohoku.ac.jp; wakao@med.tohoku.ac.jp; mdezawa@med.tohoku.ac.jp



Creative Commons Non Commercial CC BY-NC: This article is distributed under the terms of the Creative Commons Attribution-NonCommercial 4.0 License (<https://creativecommons.org/licenses/by-nc/4.0/>) which permits non-commercial use, reproduction and distribution of the work without further permission provided the original work is attributed as specified on the SAGE and Open Access pages (<https://us.sagepub.com/en-us/nam/open-access-at-sage>).

Introduction

The peripheral blood (PB) contains several types of stem/progenitor cells, including hematopoietic stem cells positive for CD34 and endothelial progenitor cells (EPCs) positive for CD31, von Willebrand factor, and VE-cadherin¹. Bone marrow (BM)-derived mesenchymal stem cells (MSCs), which are normally very sparse in the PB, are mobilized into the PB in some situations².

Multilineage-differentiating stress-enduring (Muse) cells are endogenous nontumorigenic pluripotent-like stem cells positive for pluripotent markers, including Nanog, Oct3/4, and Sox2, that generate endodermal-, ectodermal-, and mesodermal-lineage cells from single cells and self-renew^{3–7}. Muse cells are stress-tolerant, have high activity to repair damaged DNA, exhibit low telomerase activity, and do not form teratomas when transplanted *in vivo*^{3–7}. They are identified as cells positive for stage-specific embryonic antigen (SSEA)-3, a pluripotent surface marker, in the PB, BM, and organ connective tissues^{4,8–10}.

Muse cells exhibit unique characteristics *in vivo*. Muse cells express sphingosine-1-phosphate (S1P) receptor 2 (S1PR2) and sense the S1P produced by damaged tissue, which enables them to migrate to and home to the site of tissue damage¹¹. Therefore, Muse cells, in both the circulation and tissues, can selectively accumulate at the damaged site. After homing, Muse cells spontaneously differentiate into tissue-constituent cells and replenish damaged/lost cells to participate in tissue repair, as demonstrated following intravenous injection of exogenous Muse cells into animal models of stroke, encephalitis, acute myocardial infarction, renal failure, and liver damage^{11–15}. Clinical data from patients with acute myocardial infarction and stroke indicate that the serum S1P levels increase prior to the increase in the number of endogenous PB-Muse cells after onset and this increase in the acute phase significantly correlates with functional recovery at 6 months, supporting a reparative function of Muse cells *in vivo*^{11,16}.

Those 'PB-Muse cells' were analyzed only on the basis of their SSEA-3-positivity and their properties have not been characterized. In the present study, we collected SSEA-3(+) cells from the PB of healthy volunteers and compared them with BM-derived Muse cells (hereafter referred to as BM-Muse cells) as representative tissue-derived Muse cells, as well as with PB-derived SSEA-3(-)-mononuclear cells.

Materials and Methods

Isolation of Human PB-derived SSEA-3(+) Cells

Approximately 20 ml of PB from a healthy volunteer was collected into a collection tube containing ethylenediaminetetraacetic acid (EDTA). To isolate mononuclear cells, an equal volume of Dulbecco's phosphate-buffered saline with 2% fetal bovine serum (FBS, STEMCELL Technologies, Vancouver, BC, Canada) was added to the blood and the diluted blood was layered over the septum of a SepMate-

50 tube (STEMCELL Technologies) filled with Lymphoprep (STEMCELL Technologies) under the septum, and centrifuged at 1,200 g for 20 min at room temperature. The specific gravity centrifugation method was performed according to the manufacturer's protocol. Approximately, $8 \sim 14 \times 10^6$ mononuclear cells were collected in each sample. The isolated mononuclear cells were then resuspended at a concentration of 1×10^6 cells/100 μ l in fluorescence-activated cell sorting (FACS) buffer containing FluoroBrite Dulbecco's Modified Eagle Media (DMEM; Thermo Fisher Scientific, Pittsburgh, PA, USA), 100 mM EDTA, and 5% bovine serum albumin, and then incubated with 10% inactivated human AB type serum for 20 min at 4°C for Fc receptor blocking. After filtration through a 40- μ m FALCON Cell Strainer (Corning, Corning, NY, USA), anti-SSEA-3 antibody (1:100; BioLegend, San Diego, CA, USA) was added and the cells were incubated for 60 min in the dark at 4°C with gentle mixing every 10 min. The cells were then washed three times with FACS buffer. Next, fluorescein isothiocyanate (FITC)-labeled anti-rat IgM antibody (1:100; Jackson ImmunoResearch, West Grove, PA, USA) was added as a secondary antibody and the cells were incubated for 60 min in the dark at 4°C with gentle mixing every 10 min. Cells were then washed three times with FACS buffer. Finally, Hoechst33342 (Invitrogen, Eugene, OR, USA) was added for nuclear staining and the cells were incubated for 30 min at room temperature to distinguish mononuclear cells from erythrocytes. FACS (FACS Aria II, Becton Dickinson, San Jose, CA, USA) and FACSDiva Software (Becton Dickinson) were used for analysis and isolation. Cells without any antibody incubation, cells incubated with only secondary antibody (FITC-labeled anti-rat IgM antibody), and cells incubated with rat IgM (1:100; BioLegend) followed by the secondary antibody (FITC-labeled anti-rat IgM antibody) as an isotype control were used to exclude the nonspecific reactions and auto-fluorescence, as well as to set the gate for the SSEA-3(+) cells. The procedure is shown in Fig. 1.

The proportion of SSEA-3(+) cells to mononuclear cells was calculated according to the SSEA-3(+) cell number/Hoechst33342(+) cell number \times 100 (%). The number of SSEA-3(+) cells is presented as absolute number per 1×10^5 cell counts of PB-mononuclear cells. For viability staining, samples incubated with primary (SSEA-3) and secondary (FITC-rat IgM) antibodies were finally incubated with Hoechst 33342 in the presence of 7-amino-actinomycin D (7-AAD, 1:20; BioLegend) and then subjected to FACS analysis.

Laser Confocal Microscopy of Human PB-Derived SSEA-3(+) Cells

Human PB-derived SSEA-3(+) cells, hereafter referred to as PB-SSEA-3(+) cells, were placed on a slide glass immediately after isolation by FACS and observed with a laser

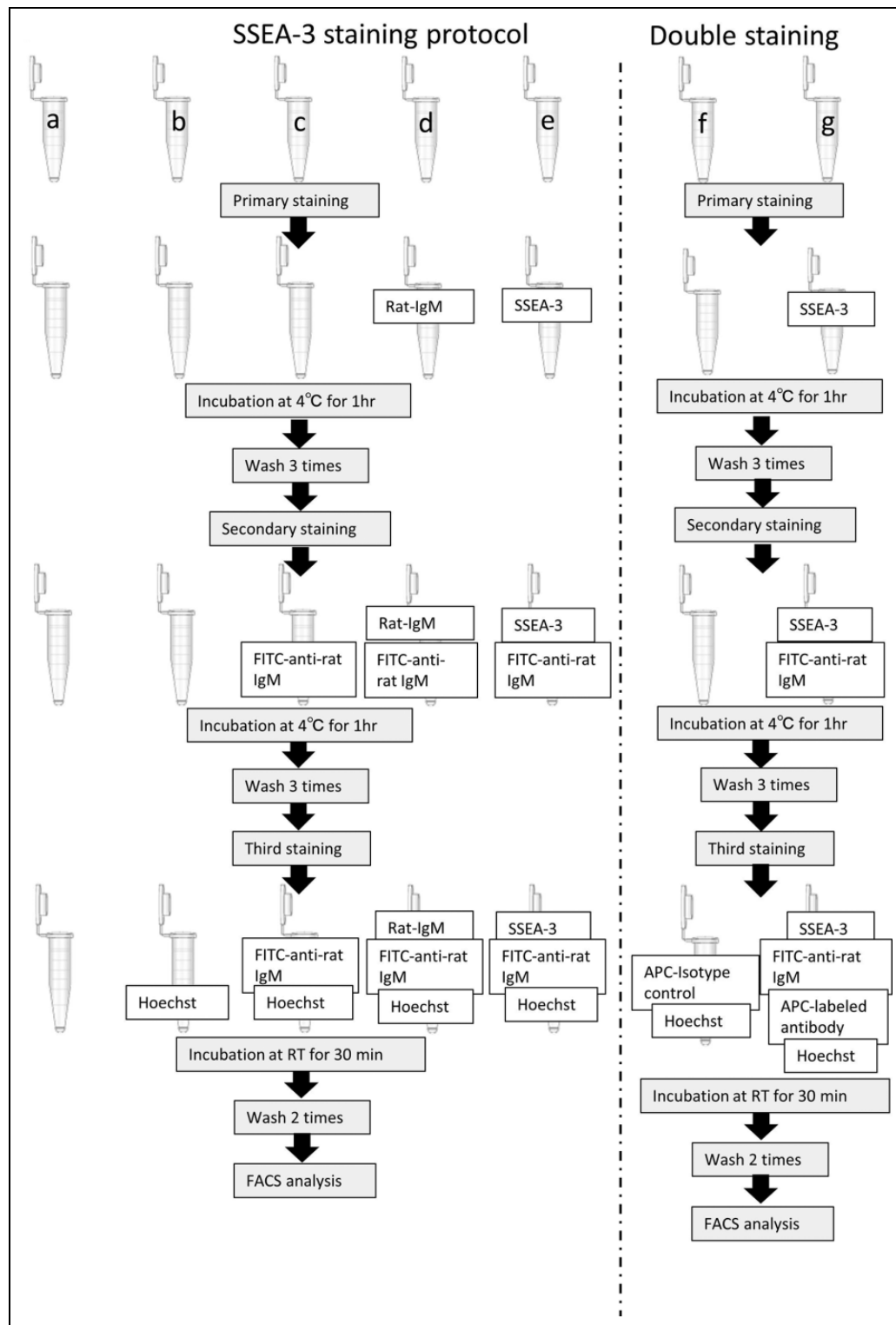


Fig. 1. Protocol for FACS analysis. The staining method for isolating human PB-SSEA-3(+) cells from PB-mononuclear cells using anti-SSEA-3 antibody is shown on the left side (SSEA-3 staining protocol). In this method, mononuclear cells isolated using Lymphoprep were dispensed at 1×10^6 cells into each of five tubes (a–e), and anti-SSEA-3 antibody (e) and rat-IgM (d) (isotype control) were added to two tubes (d and e, respectively), and then these two tubes were incubated at 4°C for 1 h with mixing every 10 min, followed by three washes. The secondary antibody for SSEA-3, FITC-anti-rat IgM antibody, was then added to the above two samples (d and e) and one new tube (for secondary antibody only) (c). After repeating the incubation and washing regimen, Hoechst 33342 for nuclear staining was added to the above three samples (c–e) and one new tube (for Hoechst 33342 staining only) (b) and incubated at room temperature for 30 min, washed twice, and

(to be Continued.)

confocal microscope (C2si; Nikon Corporation, Tokyo, Japan).

Double-Staining of PB-SSEA-3(+) Cells in Flow Cytometry

Approximately 10–20 ml fresh PB was obtained from four healthy volunteers. After staining for SSEA-3, the cells were further stained with another marker for double-staining. The positive cell population gates were set using two isotype controls, mouse IgG1 κ and mouse IgG2 α κ , both directly labeled with allophycocyanin (APC). The proportion of double-positive cells was calculated according to the number of double-positive cells/number of SSEA-3(+) cells \times 100 (%). Antibodies used for double-staining with SSEA-3 were APC-labeled mouse anti-human -CD2, -CD14, -CD16, -CD19, -CD34, -CD45, -CD62P, -CD62E, -CD73, -CD105, -CD106, and -HLA-DR (at 1:20 dilution, all purchased from Becton Dickinson), and APC-labeled mouse anti-human -CD144, -CD309 (at 1:20 dilution, both purchased from BioLegend). The collected PB-mononuclear cells were divided into 21 tubes, each containing $\sim 1 \times 10^6$ PB-mononuclear cells, and subjected to either no stain, Hoechst 33342 only, rat IgM secondary antibody only, isotype control for rat IgM, isotype controls for mouse IgG1 κ and mouse IgG2 α κ , SSEA-3 staining only, or double-staining for SSEA-3 plus the above-mentioned 14 markers. The detailed incubation protocol is described in Fig. 1.

Analysis of Fresh Human BM-Muse Cells

Approximately 15 ml of human fresh unprocessed BM aspirates was purchased from Lonza (Lonza Inc., Allendale, NJ, USA). SSEA-3(+) cells were isolated using the same protocol as described above with minor modifications. Various types of nucleated red blood cell-lineage cells were contained in the BM, for example, pre-erythroblasts, basophilic erythroblasts, and polychromatic erythroblasts. For this, the erythrocytes were removed by hemolysis with ACK Lysis Buffer (1.5 mM NH₄Cl, 0.1 mM KHCO₃, and 0.01 mM Na₂EDTA) instead of Hoechst33342 nuclear staining. After incubation with the SSEA-3 antibody followed by FITC-labeled anti-rat IgM antibody, the cells were incubated with either APC-labeled anti-CD45 or anti-CD105 antibodies for 30 min at room temperature and

analyzed. APC-labeled mouse IgG1 κ was used as an isotype control.

Quantitative Polymerase Chain Reaction

Approximately 6,000 PB-SSEA-3(+) and PB-SSEA-3(-) cells were collected from two healthy volunteers and $\sim 6,000$ Muse cells were collected from human BM-MSCs (Lonza Inc., Basel, Switzerland) as SSEA-3(+) cells, as mentioned above³. Total ribonucleic acid (RNA) was extracted and purified from these cells using NucleoSpin RNA XS (Macherey-Nagel, Bethlehem, PA, USA), and subjected to reverse transcription to obtain complementary DNA (cDNA) using a SuperScript III synthesis kit (Invitrogen) according to the manufacturer's instructions. The samples were applied to an Applied Biosystems 7500 fast real-time PCR system (Applied Biosystems, Carlsbad, CA, USA) for quantitative polymerase chain reaction (Q-PCR). The cDNA was reacted with Taqman Universal Master Mix II with UNG (Applied Biosystems) for Nanog, OCT4, Sox2, S1PR1, S1PR3, S1PR4, S1PR5, CD105, and CD45, or with SYBR Green PCR Master Mix (Applied Biosystems) for S1PR2. The data were analyzed using the $\Delta\Delta C_t$ method from the obtained C_t value, and the results are presented as fold-change of gene expression¹⁷. The following primer/probe set was purchased from Applied Biosystems: β -actin (Hs99999903_m1), Nanog (Hs04260366_g1), OCT4 (Hs00999632_g1), SOX2 (Hs01053049_s1), S1PR1 (Hs01922614_s1), S1PR3 (Hs00245464_s1), S1PR4 (Hs02330084_s1), S1PR5 (Hs00928195_s1), CD45 (Hs00236304_m1), and CD105 (Hs00923996_m1). The specific primer sets for S1PR2 were as follows: forward primer 5'-ACCTCAAGTGATCCGCC-3' and reverse primer 5'-CTAGCCACTGCCACCCC-3'.

PB-SSEA-3(+) Cell Culture

The following methods were used to culture and proliferate PB-SSEA-3(+) cells: (1) $\sim 10 \times 10^3$ cells were plated onto a 96 well-culture dish per well (Corning) and cultured in DMEM with 10% FBS at 37°C, 5% CO₂. For tracing, cells were labeled with Hoechst 33342 and vibrant CFDA-SE cell tracer (ThermoFisher). (2) $\sim 10 \times 10^3$ cells were plated onto a fibronectin-coated 96 well-culture dish per well (Corning) and cultured in DMEM with 10% human serum (pool of donors; BioIVT, Westbury, NY, USA). (3) $\sim 10 \times 10^3$ cells

Fig. 1. (Continued). analyzed by FACS. The last tube was directly analyzed without any stain (nonstained) (a) for forward scatter (FSC), side scatter (SSC), and the removal of doublet cells. A method for double staining, SSEA-3 plus each marker, is shown on the right side (double staining). Two tubes (f and g) were prepared, and one was stained with anti-SSEA-3 and FITC-anti-rat IgM antibodies (g) as mentioned above, and then the third incubation step was performed, namely incubation with APC-labeled mouse anti-human -CD2, -CD14, -CD16, -CD19, -CD34, -CD45, -CD62P, -CD62E, -CD73, -CD105, -CD106, -HLA-DR, -CD144, or -CD309, in the presence of Hoechst 33342 (g). Another tube was used for the APC-labeled isotype control antibody and Hoechst 33342 incubation (f). The use of APC-labeled direct antibody and isotype control was performed according to the manufacturer's instructions. FACS: fluorescence-activated cell sorting; APC: allophycocyanin.

were plated into each well of a fibronectin-coated 96 well-culture dish (Corning) and cultured in DMEM with 5% FBS and 5% inter- α -inhibitor, known to promote attachment and long-term growth of pluripotent stem cells such as embryonic stem cells by activating Yes/YAP/TEAD transcription pathway¹⁸ (Athens Research And Technology, Inc., Athens, GA, USA). (4) MethoCult (H4100; STEMCELL Technologies) was diluted in 20% (vol/vol) FBS plus α -minimal essential medium to a final concentration of 0.9%. MethoCult (100 μ l) was placed into each well of a 96-well plate (Corning), $\sim 10 \times 10^3$ cells were seeded on the top of MethoCult, and then another 50 μ l MethoCult was added. The cells and MethoCult were mixed thoroughly by gentle pipetting and cultured at 37°C, 5% CO₂. To change the medium, 10% of the volume of the initial MethoCult culture medium was gently added to the wells every 3 d.

Migration Assay

To analyze the migration of human PB-SSEA-3(+) cells, a chemotaxis assay was performed using a IncuCyte ClearView 96-well Cell Migration Plate (Essen Bioscience, Ann Arbor, MI, USA) according to the manufacturer's protocol. The plate was coated with Protein-G (Life Technologies, Carlsbad, CA, USA) and ICAM-1 (Life Technologies) according to the manufacturer's protocol. The well of the upper insert plate was seeded with ~ 500 cells in RPMI 1640 Medium (Life Technologies) containing 0.5% FBS (MilliporeSigma, St. Louis, MO, USA), and the lower reservoir plate was filled with 1.5 μ M S1P (Enamine LLC, Monmouth Jct., NJ, USA) in the same medium. Using the IncuCyte ZOOM System (Essen BioScience), time-lapse photography was performed for 12 h every 3 min at 37°C in 5% CO₂. Because the human PB-SSEA-3(+) cells were not adherent *in vitro*, the number of cells at the bottom of the reservoir plate below the pore of the wells of the insert plate could not be measured as for adhesive cells. PB-SSEA-3(+) cells were collected from one donor. The migration distance, velocity, and directionality¹⁹ of the cells on the insert plate were evaluated using Chemotaxis software, which is a plug-in function of ImageJ software (National Institutes of Health, Bethesda, MD, USA), and compared with those of the PB-SSEA-3(+) cells whose lower reservoir plate contained medium without S1P. For evaluation, single cells that were observed to migrate were randomly selected, and their trajectories were manually traced and analyzed using ImageJ software.

Administration of Human PB-SSEA-3(+) Cells to Mouse Damaged Tissues

All the animal experiments were done under deep anesthesia with 1.5% isoflurane. A lacunar stroke mouse model was created according to previous reports¹³. In brief, vasoconstrictive peptides, endothlin-1 combined with the nitric oxide synthase inhibitor N(G)-nitro-L-arginine methyl ester, were

injected into the right internal capsule of a male SCID mouse (10 wk old) to induce a lacunar infarction. After 1 wk, 600~800 human PB-SSEA-3(+) cells isolated by FACS from healthy donors were suspended in 3 μ l FluoroBrite DMEM and stereotaxically injected into the perilesion site (from bregma: AP, -2.0 mm; ML, +2.0 mm; DV, -3.0 mm). For muscle degeneration, cardiotoxin was injected into the gastrocnemius muscles of male C57BL/6 mice (10-wk old), according to the previous method³. Approximately 500 human PB-SSEA-3 (+) cells isolated by FACS from healthy donor PB were locally injected to the degenerated site 2 d after inducing the damage. Control received the same volume of PBS.

One week after injecting the PB-SSEA-3(+) cells in both models, the mice were perfused intracardially with periodate lysine paraformaldehyde solution (0.01 M NaIO₄, 0.075 M lysine, and 2% paraformaldehyde, pH 6.2). The brains and muscles of injected region were dissected out and postfixed in the same fixative for at least 6 h at 4°C.

For the liver, male C57BL/6 mice (10-wk old) liver was dissected out under anesthesia and tissue slices at 2-mm thick were prepared and placed on culture dishes. Then, ~ 500 human PB-SSEA-3 (+) cells were supplied onto the liver slice. Culture media contained DMEM, GlutaMAX (Gibco), 0.1 mg/ml kanamycin sulfate (Gibco), and 10% fetus bovine serum, and samples were cultured in 5% CO₂ at 37°C. Three days after, liver slices were fixed with 4% paraformaldehyde in 0.02 M PBS.

The fixed samples were cryoprotected by successive immersion into 15%, 20%, and 25% sucrose overnight at 4°C, embedded in O.C.T. compound (Sakura Finetek USA, Inc., Torrance, CA, USA), and cut into 6- μ m thick sections using a cryostat (CM1850; Leica, Wetzlar, Germany). Cryosections were blocked with blocking buffer (20% Block Ace, 5% bovine serum albumin, 0.3% Triton X-100, and PBS) for 30 min at room temperature. For the brain tissue, samples were then incubated with the anti-human mitochondria antibody (1:100; Merck Millipore, Darmstadt, Germany) at 4°C overnight, and then sections were incubated with Alexa 488-labeled antimouse IgG antibody (1:500; Jackson ImmunoResearch) as the secondary antibody for 2 h at room temperature. The sections were then further incubated with anti-NeuN antibody (1:100; Abcam, Cambridge, MA, USA) followed by Alexa 680-labeled antirabbit IgG antibody (1:500; Invitrogen), and then counterstained with 4',6-diamidino-2-phenylindole (1:1000; MilliporeSigma).

For the muscle tissue, primary antibodies used were anti-human Golgi complex antibody (1:200; Abcam), anti-Desmin antibody (1:100, BD Pharmingen) and anti-Pax7 antibody (1:200; DSHB, University of Iowa). For the liver tissue, primary antibodies used were human mitochondria antibody (1:100), antialpha-fetoprotein antibody (1:10, DAKO, Santa Clara, CA, USA), and anticytokeratin 19 (CK19) antibody (1:100, SantaCruz, Dallas, Texas, USA). After washing with PBS, samples from the muscle and liver were incubated with secondary antibodies either of

antimouse IgG antibody conjugated with Alexa 568 or anti-rabbit IgG antibody conjugated with Alexa-488 under the presence of DAPI in the antibody diluents for 2 h at room temperature. For control, staining without primary antibodies was performed.

Samples were inspected using a laser confocal microscope (A1 R; Nikon Corporation). For counting human-mitochondria(+) and human-Golgi complex(+) cells, five fields were randomly selected from areas near the injection site and the positive cells were counted.

Statistical Analysis

Data are expressed as the mean \pm standard error (SE). Student's *t*-test was applied to assess the significance of differences between two groups. Statistical analysis was performed with JMP statistical software (SAS Institute, Cary, NC, USA). A value of $P < 0.05$ was considered statistically significant.

Results

Analysis of PB-SSEA-3(+) Cells

Tissue-derived Muse cells are labeled and identified as SSEA-3(+), as previously reported^{3,5,8,10}. SSEA-3(+) cells are also observed to increase in the PB of patients with stroke and acute myocardial infarction^{11,16}. In this study, we therefore collected SSEA-3(+) cells from human PB for analysis.

Fresh PB samples obtained from 16 healthy volunteers (mean age: 36.7 ± 2.1 years, eight men and eight women) without remarkable past medical histories were used in the study. We carefully identified the SSEA-3(+) cells using multiple controls by setting strict gates for FACS. The experimental procedure is shown in Fig. 1 and an example of the analysis of SSEA-3(+) cells among PB-mononuclear cells is shown in Fig. 2A–H. First, the mononuclear cell fraction after Lymphoprep treatment was roughly selected by forward scatter and side scatter (Fig. 2A), doublet cells were removed (Fig. 2B), and the few remaining red blood cells, negative for Hoechst 33342, were removed by specific gravity centrifugal methods (Fig. 2C). Nonspecifically labeled cells were removed based on secondary antibody-only staining (Fig. 2D) as well as isotype control (Fig. 2E), and finally the gating was set for SSEA-3(+) cells (Fig. 2F). In the example shown in Fig. 2F, PB-SSEA-3(+) cells comprised $0.04\% \pm 0.003\%$ of total PB-mononuclear cells. To confirm whether dead cells had contaminated the PB-SSEA-3(+) fraction, PB-mononuclear cells were stained with both SSEA-3 and 7-AAD (a dead cell marker). While $0.36\% \pm 0.03\%$ of the PB-mononuclear cells comprised 7-AAD(+) cells, none of the SSEA-3(+) cells was 7-AAD(+) (Fig. 2G, H). Isolated PB-SSEA-3(+) cells were confirmed to contain a nucleus and their surface was labeled by the green fluorescence of the SSEA-3 marker under laser confocal microscopy. The mean diameter of the PB-SSEA-3(+) cells was $10.1 \pm 0.3 \mu\text{m}$ (range: 8.7–14.7 μm ; Fig. 2I).

We further analyzed fresh PB from 15 volunteers using the same method (Fig. 2J, K). The mean proportion of PB-SSEA-3(+) cells among the total PB-mononuclear cells was $0.04\% \pm 0.01\%$, while the percentage varied among individuals (Fig. 2K).

To further characterize PB-SSEA-3(+) cells, surface marker expression was examined in four healthy volunteers (Donors #1, 2, 3, and 8 in Fig. 2K). Tissue-derived Muse cells, for example from the BM, adipose tissue, and dermis, are reported to be double positive for SSEA-3 and mesenchymal marker CD105^{3,8}. The ratio of PB-SSEA-3(+) cells positive for CD105 was only $22.4\% \pm 3.8\%$ and the ratio of PB-SSEA-3(+) cells positive for CD73, another MSC marker, was $47.5\% \pm 6.5\%$ (Fig. 3A–C). We then examined blood cell-lineage markers CD2 (T cells and NK cells), CD14 (monocyte-lineage cells), CD16 (NK cells and monocyte-lineage cells), CD19 (B-cells and follicular dendritic cells), and CD45 (white blood cells); hematopoietic stem cell marker CD34; endothelial progenitor cell markers CD309 (vascular endothelial growth factor receptor-2 [VEGFR-2]) and CD144 (VE-Cadherin); HLA-DR (major histocompatibility complex class II molecule relevant to antigen presentation); and cell adhesion molecules CD62P (P-selectin), CD62E (E-selectin), and CD106 (VCAM-1) (Fig. 3A–G, supplemental Fig. S1A–H). Interestingly, 100% of PB-SSEA-3(+) cells were positive for CD45, a leukocyte common antigen (Fig. 3D). Regarding the other blood cell-lineage markers, $84.9\% \pm 4.6\%$ of PB-SSEA-3(+) were positive for CD19, and $3.2\% \pm 1.5\%$ were positive for CD14 (Fig. 3E, F), and negative for CD2 and CD16. None of the PB-SSEA-3(+) cells was positive for CD34, CD62P, CD62E, CD106, CD144, or CD309 (supplemental Fig. S1A–H). High proportion of PB-SSEA-3(+) cells expressed HLA-DR ($93.9\% \pm 2.2\%$) (Fig. 3G).

Analysis of BM-Muse Cells

Human BM-Muse cells were directly isolated from fresh unprocessed BM aspirates using a method similar to that used for isolating the PB-SSEA-3(+) cells with the minor modification of eliminating the red blood cell-lineage cells. The mean percent of SSEA-3 in the total BM-mononuclear cells was $0.2\% \pm 0.01\%$ (Fig. 4A). We further examined the expression of CD45, which was positive in 100% of the PB-SSEA-3(+) cells, as well as CD105, which is expressed in nearly 100% of tissue-Muse cells obtained from the dermal-, adipose tissue-, and umbilical cord-derived MSCs, as SSEA-3(+) cells^{8,10}. Consequently, $7.5\% \pm 0.9\%$ of BM-Muse cells were positive for CD45 (Fig. 4B) and $68.4\% \pm 1.7\%$ were positive for CD105 (Fig. 4C).

Gene Expression and Other Properties of PB-SSEA-3(+) Cells

Fresh PB-SSEA-3(+) cells isolated from two healthy volunteers (Donors #1 and #3 in Fig. 2K) were subjected to gene

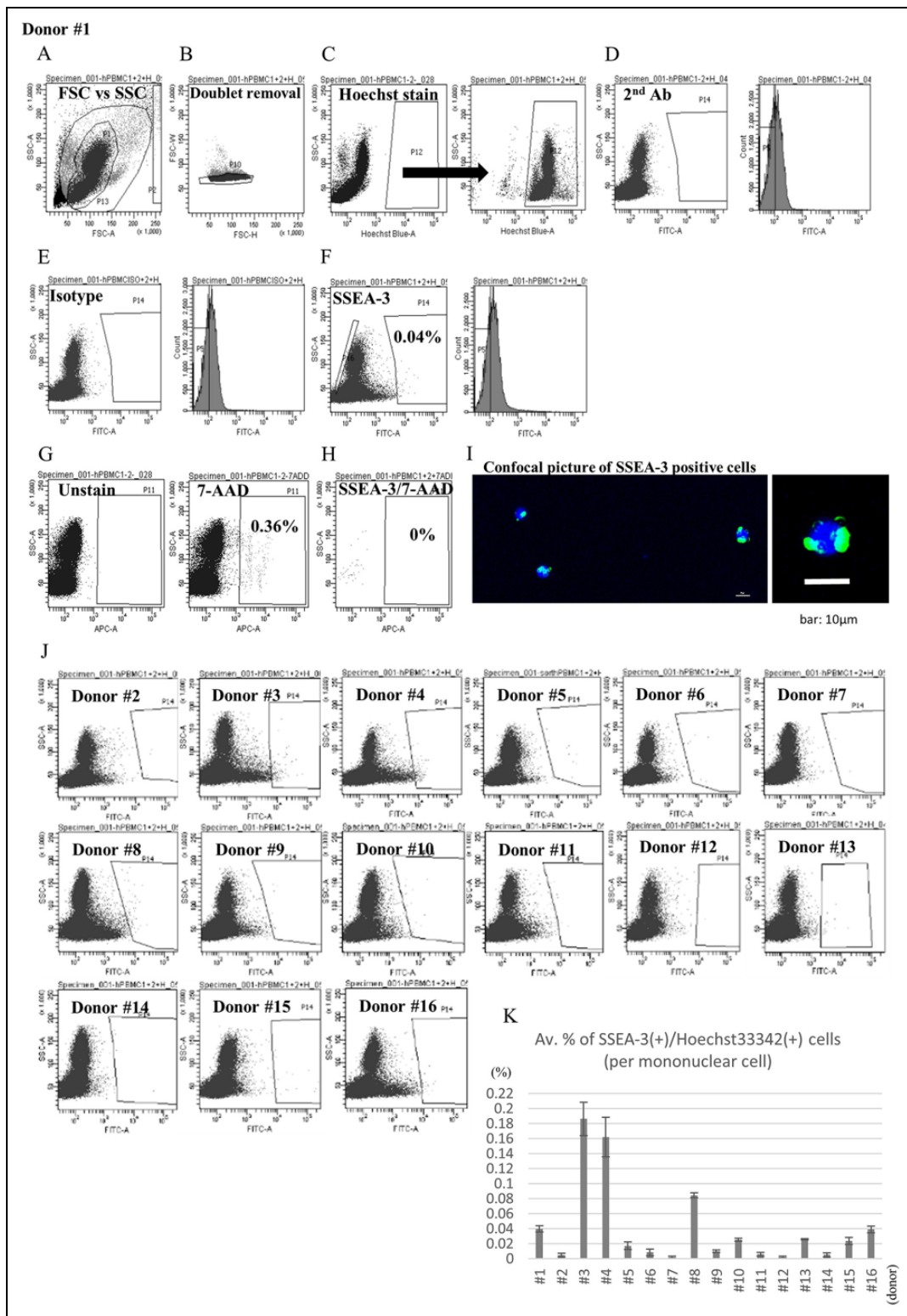


Fig. 2. SSEA-3(+)-Mouse cells in the PB of healthy volunteers. (A–F) PB-SSEA-3(+) cells in human fresh PB. (A) Rough selection of mononuclear cells after Lymphoprep by FSC vs SSC in the nonstained sample. (B) Removal of doublet cells using FSC-Width. (C) Selection of pure mononuclear cells and removal of red blood cells by Hoechst33342 staining (right side of C) from nonstained rough mononuclear cells (left side of C). (D, E) Analysis of human PB-mononuclear cells stained with secondary antibody only (FITC-labeled anti-rat IgM antibody) (D) and isotype control (rat IgM + FITC-labeled anti-rat IgM antibody) (E). (F) PB-mononuclear cells stained with anti-SSEA-3 antibody followed by secondary antibody. SSEA-3(+) cells comprised 0.04% of the PB-mononuclear cells. (G, H) Analysis of dead cells and (to be Continued.)

expression analysis (P14 in Fig. 5A). The levels of the pluripotency markers Nanog, Oct3/4, and Sox2 in PB-SSEA-3(+) cells were remarkably higher ($\sim 90x$, $\sim 30x$, and $\sim 45x$, respectively) in PB-SSEA-3(+) cells than in BM-Muse cells (Fig. 5B; all with $P < 0.01$).

The S1PR has five subtypes, S1PR1 \sim S1PR 5²⁰. S1PR1, 3, 4, and 5 gene expression levels were not significantly different between PB-SSEA-3(+) and PB-SSEA-3(-) cells (P15 in Fig. 5A), while that of S1PR2 was approximately seven times higher in PB-SSEA-3(+) cells than in PB-SSEA-3(-) cells ($P < 0.01$; Fig. 5C). We then compared the gene expression level of S1PR2 between PB-SSEA-3(+) and BM-Muse cells; S1PR2 expression was ~ 50 times higher in PB-SSEA-3(+) cells than in BM-Muse cells ($P < 0.001$; Fig. 5D).

We also examined the gene expression levels of CD105 and CD45. CD105 was ~ 0.2 times lower in PB-SSEA-3(+) cells than in PB-SSEA-3(-) cells ($P < 0.001$), while CD45 was nearly the same level in PB-SSEA-3(+) cells and PB-SSEA-3(-) cells (Fig. 5E). CD105 gene expression was also examined in PB-SSEA-3(+) and BM-Muse cells. The expression level of CD105 was 67 times lower in PB-SSEA-3(+) cells than in BM-Muse cells ($P < 0.001$; Fig. 5F).

The PB-SSEA-3(-) cell population is considered heterogeneous and comprises several subpopulations, including monocytes, lymphocytes, and other kinds of white blood cells. As shown in supplemental Fig. 2A, three subpopulations of PB-SSEA-3(-) cells, P16, P17, and P18, all of which were gated differently from those in Fig. 5A, were individually selected from the SSEA-3(-) fraction, and subjected to Q-PCR. Compared with PB-SSEA-3(+) cells, the gene expression of CD105, CD45, and S1PR2 was similar to that shown in PB-SSEA-3(-) cells in Fig. 5C–E (supplemental Fig. 2B).

Tissue-Muse cells derived from the BM, adipose tissue, dermis, and umbilical cord are reported to adhere to the culture dish without requiring a fibronectin coating and to proliferate in adherent culture^{4,8,10}. They are also reported to proliferate from a single cell to generate embryonic stem cell-derived embryoid body-like clusters in suspension culture^{3,5,8,10}. The PB-SSEA-3(+) cells, however, neither adhered to nor proliferated on the culture dish for up to 7 d under the conventional conditions as used for adherent culture of tissue-Muse cells (supplemental Figs 2C and 3). Even when the dish was coated with fibronectin, or combining fibronectin coating and administration of inter- α -inhibitor, known to promote attachment and growth of embryonic

stem cells by activating Yes/YAP/TEAD transcription factor pathway¹⁸, into the culture medium, the PB-SSEA-3(+) cells failed to adhere to the dish nor did they proliferate on the culture dish for up to 7 d (supplemental Figs 2D and 3). The cells also did not proliferate in the MethoCult suspension culture for 7 d (supplemental Fig. S3). In all cases, however, the PB-SSEA-3(+) cells did not appear to be dead (supplemental Fig. 2C and D). Therefore, single cell-derived cluster formation in suspension culture and the following triploblastic differentiation assay from clusters in adherent culture, which are generally performed in tissue-Muse cells, could not be performed in PB-SSEA-3(+) cells.

Migration of PB-SSEA-3(+) Cells to S1P

To evaluate the migration capacity of PB-SSEA-3(+) cells in the presence of S1P, a chemotaxis assay was performed by recording the movement of each PB-SSEA-3(+) cell, either with or without the presence of S1P. PB-SSEA-3(+) cells were plated in the upper insert plate, and medium with or without S1P was placed in the lower reservoir plate. Cell movement was traced and analyzed (Fig. 5G and H). The migration distance, velocity, and directionality of the PB-SSEA-3(+) cells were significantly higher when S1P was present (Fig. 5I and K).

Triploblastic Differentiation of PB-SSEA-3(+) Cells in Mouse Damaged Tissues

Topically or intravenously injected tissue-derived Muse cells are reported to selectively migrate to and integrate into sites of damage and spontaneously differentiate into tissue-compatible cells in animal disease models^{11–15}. To examine whether PB-SSEA-3(+) cells also show the same ability, freshly collected human PB-SSEA-3(+) cells were injected into a site ~ 1 mm distant from the peri-infarct region of a lacunar stroke area in a SCID mouse model at 7 d after the stroke. Immunohistochemistry of brain sections at 7 d after injecting the cells demonstrated that human PB-SSEA-3(+) cells, labeled by human-specific mitochondria, were present in the infarct region (Fig. 6A, B). Of the human mitochondria-positive PB-SSEA-3(+) cells, $33.8\% \pm 2.2\%$ expressed NeuN (Fig. 6A, B). In the mouse damaged skeletal muscle, expression of Pax7 (satellite cell marker) and desmin (skeletal muscle cell marker) were recognized in human PB-SSEA-3(+) cells, labeled by human-specific Golgi-complex at day 7 after injection (Fig. 6C, D) and $30.3\% \pm 4.1\%$ of human Golgi-complex-positive PB-SSEA-3(+) cells expressed desmin. In the mouse liver, expression of

Fig. 2. (Continued). SSEA-3(+) cells. (G) 7-AAD staining in mononuclear cells (left side of G). Dead cells comprised 0.36% of total cells. (H) Double-positive cells for SSEA-3 and 7-AAD comprised 0% of the SSEA-3(+) cells. (I) SSEA-3(+)/Hoechst33342(+) cells under a confocal laser microscope. Scale bar = 10 μ m. (J, K) SSEA-3(+) cells in fresh peripheral blood mononuclear cells from 15 healthy volunteers (J) and the proportion of the SSEA-3(+) cells to mononuclear cells in all 16 healthy volunteers (K). FSC: Forward scatter; SSC: Side scatter; 7-AAD: 7-amino-actinomycin D; PB: peripheral blood.

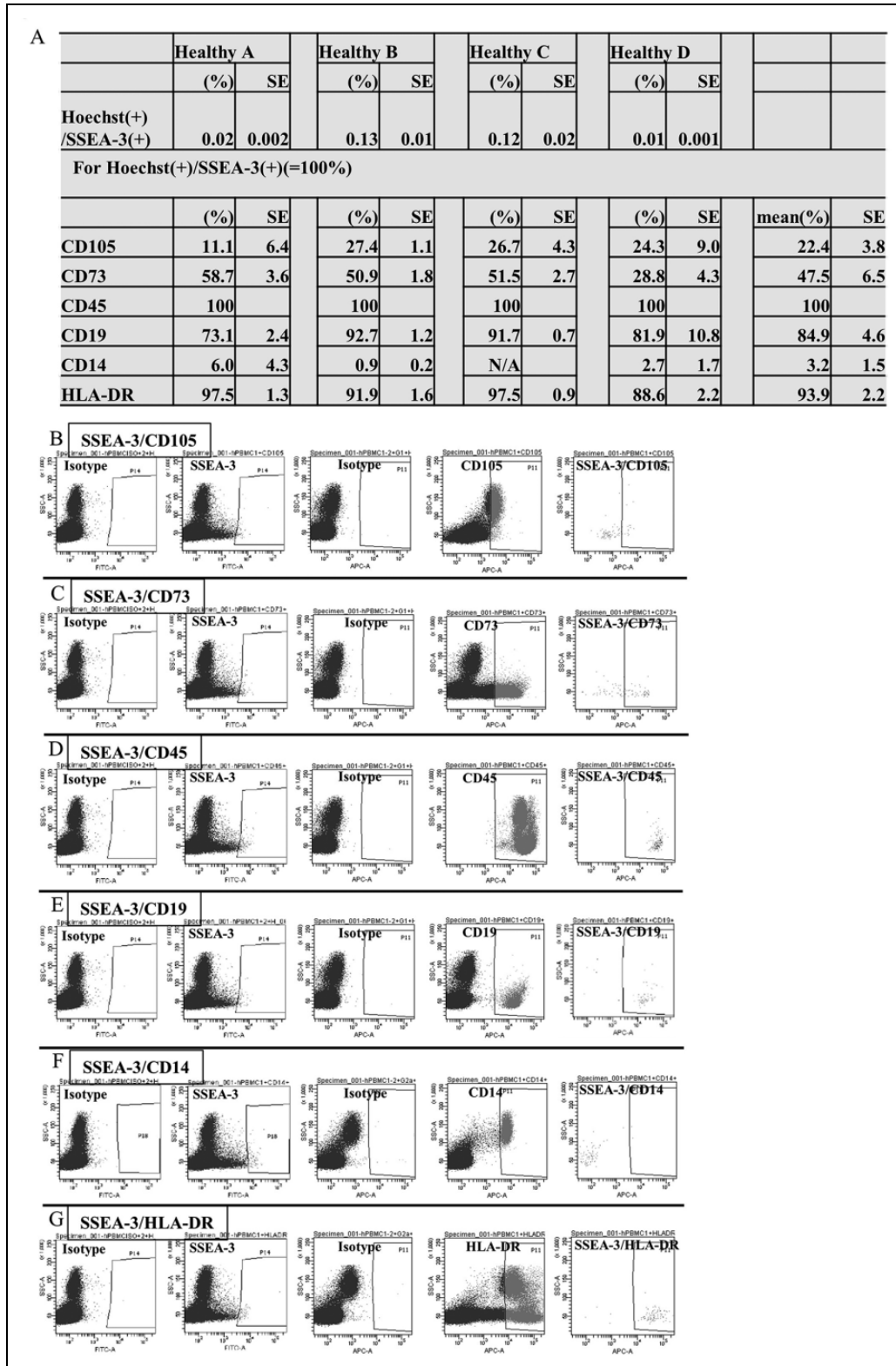


Fig. 3. Surface marker expression in PB-SSEA-3(+) cells. The proportion of SSEA-3(+)/Hoechst33342(+) cells in the PB-mononuclear cells in four healthy volunteers and the proportion of PB-SSEA-3(+) cells positive for CD105, CD73, CD45, CD19, CD14, and HLA-DR. (B–G) Examples of staining for each marker in PB-SSEA-3(+) cells. The first two figure columns on the left show the gating by the isotype control and the fraction of SSEA-3(+), respectively. The next two figure columns show the gating by the isotype control and the fraction of cells positive for (B) CD105, (C) CD73, (D) CD45, (E) CD19, (F) CD14, or (G) HLA-DR. Appropriate positive gates were set in the dot plot using the appropriate isotype control for each primary antibody. The last figure column on the right shows the fraction of cells double-positive for SSEA-3 and each marker. Data for CD2, CD16, CD34, CD62P, CD62E, CD106, CD144, and CD309, all of which were negative in PB-SSEA-3(+) cells, are shown in supplemental Fig. S1. PB: peripheral blood.

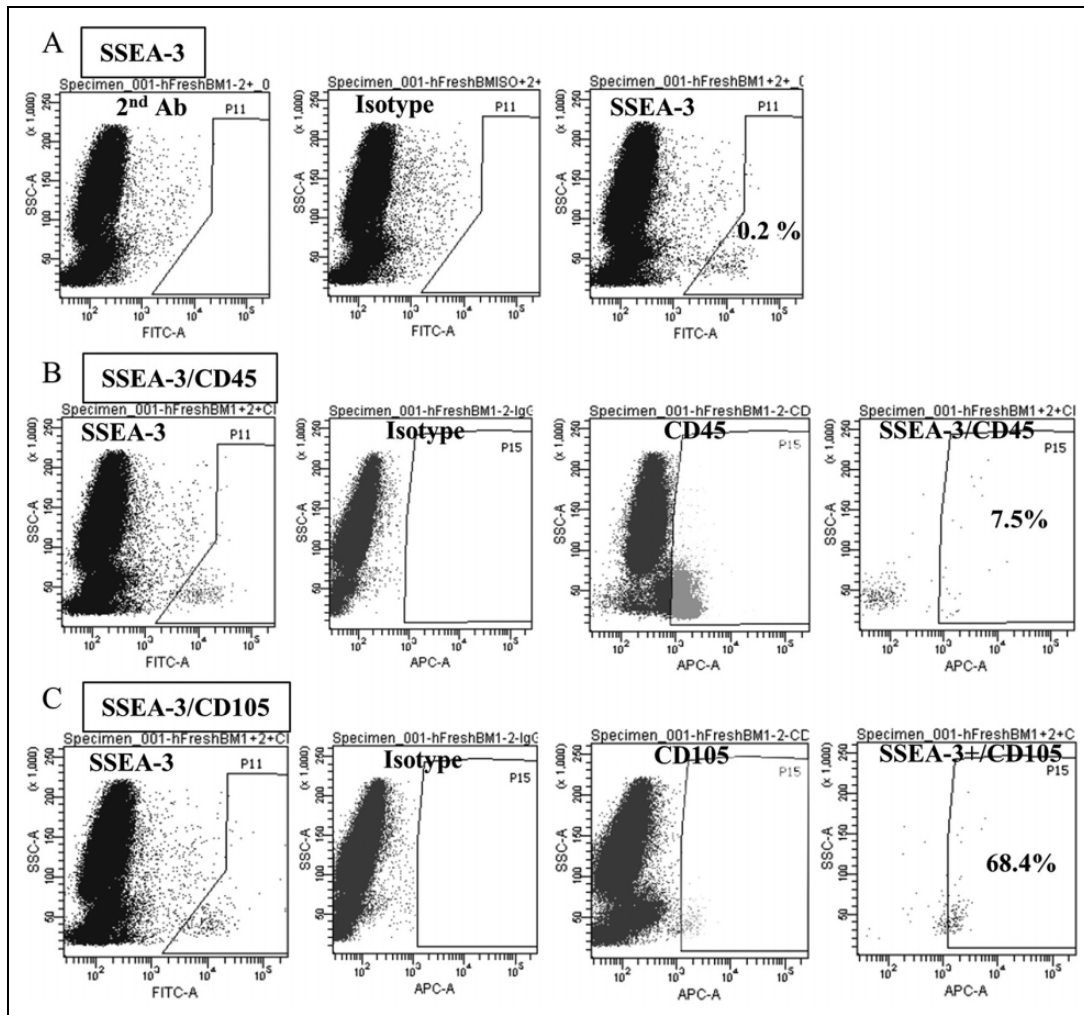


Fig. 4. Analysis of fresh BM-Muse cells. (A) Human fresh BM-mononuclear cells stained with a secondary antibody (FITC-labeled anti-rat IgM antibody) only, isotype control (rat IgM + FITC-labeled anti-rat IgM antibody) followed by secondary antibody, and anti-SSEA-3 antibody followed by secondary antibody. SSEA-3(+) was $0.2 \pm 0.01\%$. (B) SSEA-3(+) cells, isotype control for CD45 and CD45(+) cells in the BM-mononuclear cells are shown in the first three figure columns from the left. The figure column on the right shows the percent ($7.5 \pm 0.9\%$) of SSEA-3(+)/CD45(+) cells in the BM-SSEA-3(+) cells. (C) CD105 staining was performed in the same manner as in (B) and $68.4 \pm 1.7\%$ of BM-SSEA-3(+) cells were SSEA-3(+)/CD105(+). BM: bone marrow.

alpha-fetoprotein and cytokeratin-19 (both liver progenitor markers) was observed in PB-SSEA-3(+) cells, identified as human-specific mitochondria (+) cells, and $31.8\% \pm 6.2\%$ of human mitochondria-positive PB-SSEA-3(+) cells were positive for alpha-fetoprotein (Fig. 6E, F). In control samples which received PBS, we detected no human-specific mitochondria- or human-specific Golgi-complex-positive cells (data not shown).

Discussion

This study revealed the presence of stem cells in the PB that are double-positive for SSEA-3 and CD45 at a proportion of $0.04\% \pm 0.01\%$ of the total number of mononuclear cells. These cells were also positive for other pluripotent markers,

Nanog, Oct3/4, and Sox2, at significantly higher levels than in BM-Muse cells.

Like BM-Muse cells, PB-SSEA-3(+) cells expressed S1PR2 and migrated toward S1P. S1P is a lipid mediator that modulates a variety of biologic actions, including cell migration²¹. The production of S1P phosphatase and S1P lyase is increased in damaged tissue, which leads to an increase in S1P locally and generates an S1P gradient that acts to attract stem cells such as lymphocytes²². In patients with acute myocardial infarction, the increase in serum S1P occurs before the increase in endogenous SSEA-3(+) cells in the PB after the onset of acute myocardial infarction¹⁷, and Muse cells selectively home to the postinfarct cardiac tissue via S1PR2 in a rabbit model of acute myocardial infarction¹¹. Here, we demonstrated that S1PR2 gene expression

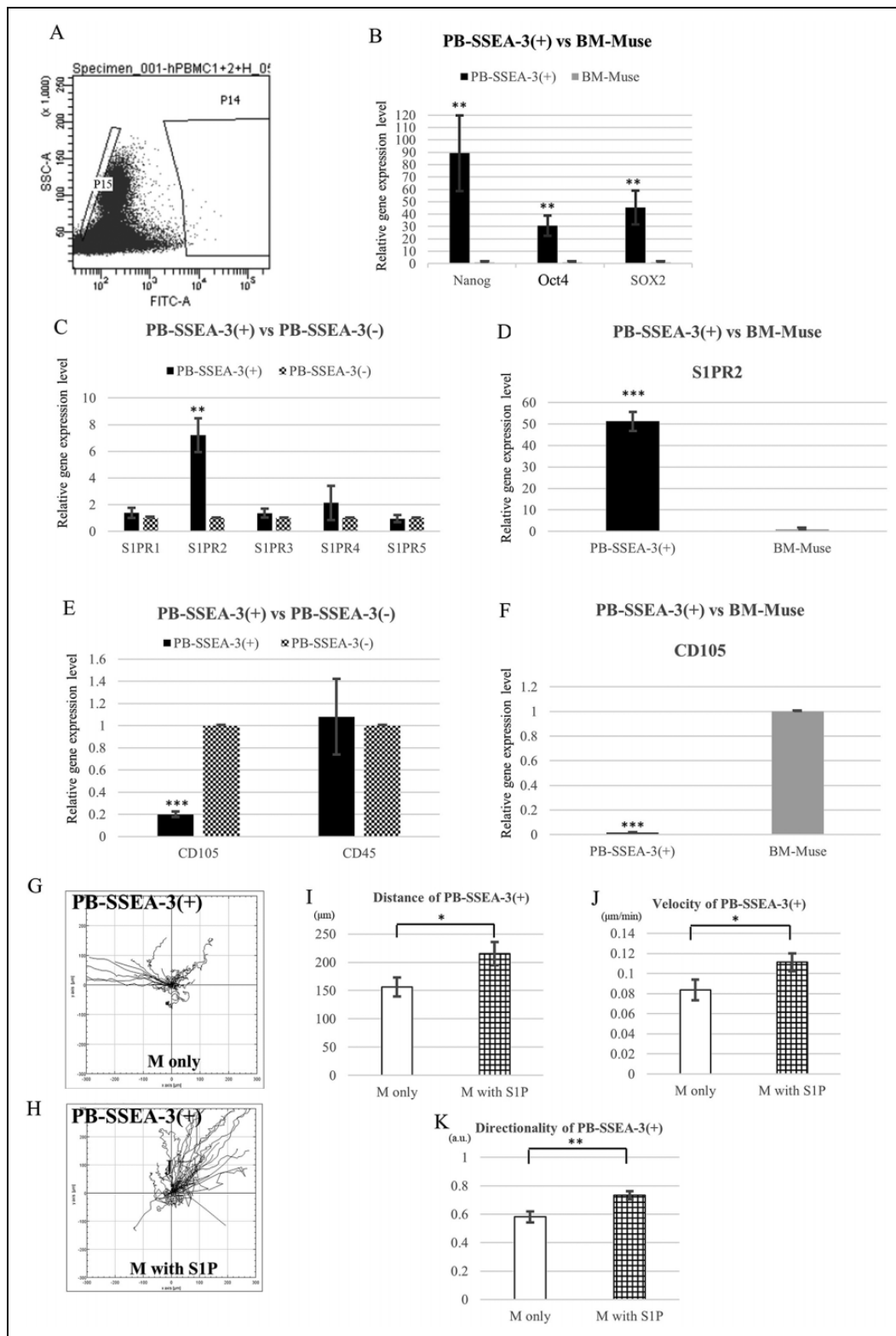


Fig. 5. Gene expression and migration assay in PB-SSEA-3(+) cells. (A) PB-SSEA-3(+) (P14 fraction) and PB-SSEA-3(-) cells (P15 fraction) were isolated from PB-mononuclear cells. (B–G) Q-PCR analysis. Nanog, OCT4, and SOX2 gene expression levels in PB-SSEA-3(+) vs BM-Muse cells (B) are shown. S1PR1–S1PR5 in PB-SSEA-3(+) vs PB-SSEA-3(-) cells (C) and S1PR2 in PB-SSEA-3(+) vs BM-Muse cells (D), CD105 and CD45 expression in PB-SSEA-3(+) vs PB-SSEA-3(-) cells (E) and CD105 expression in PB-SSEA-3(+) vs BM-Muse cells (F) are shown. Values of BM-Muse cells (B, D, and F) and PB-SSEA-3(-) cells (C, E) were set as 1 and the relative gene expression levels in PB-SSEA-3(+) cells were calculated. (G, H) Chemotaxis assay. The track of PB-SSEA-3(+) cell movement was manually traced in medium alone (G) and in medium with 1.5 μ M SIP (H). (I, K) A statistically significant difference was detected in the distance (I), velocity (J), and directionality (K) of the migration of the traced PB-SSEA-3(+) cells compared with those in medium without SIP. PB: peripheral blood; Q-PCR: quantitative polymerase chain reaction; M: medium; a.u.: arbitrary unit. *: $P < 0.05$, **: $P < 0.01$, ***: $P < 0.001$.

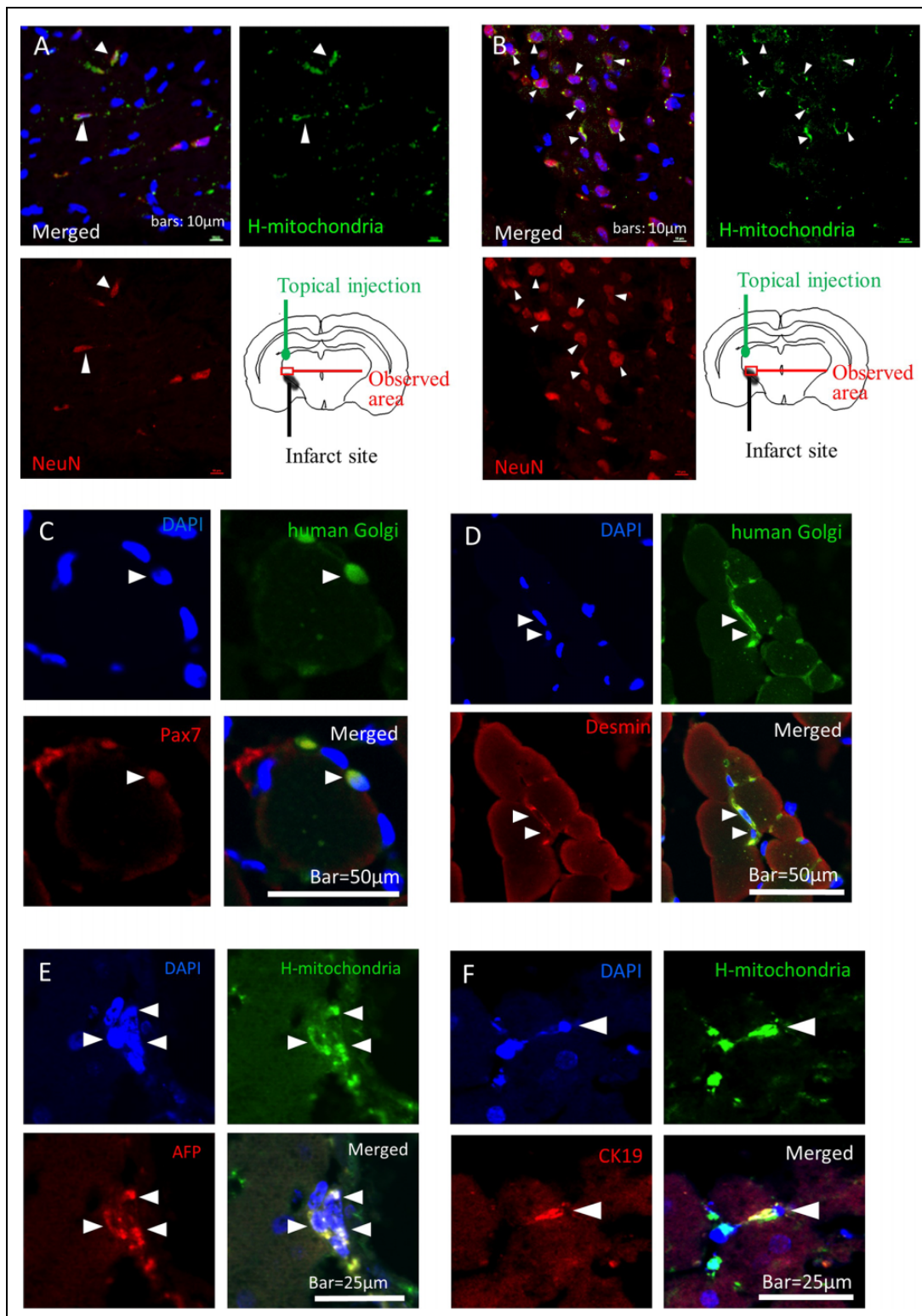


Fig. 6. PB-SSEA-3(+) cells in the damaged tissues. (A, B) Immunohistochemical staining of the brain in a mouse lacunar infarct model 7 d after injecting human PB-SSEA-3(+) cells. Human mitochondria (green)-positive cells, indicating human PB-SSEA-3(+) cells, were detected in the vicinity of the infarct lesion. Neuronal marker NeuN (red)-positive cells were identified among human mitochondria-positive cells (arrowheads). Scale bars = 10 μ m. (C, D) In damaged muscle tissue, human PB-SSEA-3(+) cells, positive for human Golgi-complex, expressed satellite cell marker Pax7 (C) and muscle cell marker desmin (D) (arrowheads). Scale bars = 50 μ m. (E, F) In the liver, human PB-SSEA-3(+) cells, positive for human mitochondria, expressed alpha-fetoprotein (AFP) (E) and cytokerain-19 (CK19) (F), both liver progenitor cell markers (arrowheads). Scale bars = 25 μ m. PB: peripheral blood.

in PB-SSEA-3(+) cells was ~50 times higher than that in BM-Muse cells. Compared with the baseline values, PB-SSEA-3(+) cells supplied with S1P exhibited a significantly greater migration distance, velocity, and directionality. Together, these findings suggest that S1P mobilizes PB-SSEA-3(+) cells.

When injected near the postinfarct area in a mouse lacunar stroke model, ~34% of topically injected human PB-SSEA-3(+) cells expressed the neuronal marker NeuN at 7 d after administration. Similarly, in a mouse lacunar stroke model, locally and intravenously injected human BM- and dermal-Muse cells integrate into the postinfarct tissue and spontaneously differentiate into cells positive for several neuronal markers, including NeuN, at 7 d after administration^{12,13,23}. In the damaged muscle tissue, locally injected human PB-SSEA-3(+) cells expressed satellite cell marker Pax7 and muscle cell marker desmin at 7 d, similar to the spontaneous differentiation of intravenously injected human BM-Muse cells in the mouse muscle degeneration model³. In the liver tissue, human PB-SSEA-3(+) cells were found to express liver progenitor markers alpha-fetoprotein and cytokeratin-19 at day 3, similar to the expression of liver progenitor markers including alpha-fetoprotein and cytokeratin-19 in human BM-Muse cells integrated into the liver 2 d after intravenous injection into mouse partial hepatectomy model²⁴. In this manner, PB-SSEA-3(+) cells are able to differentiate into ectodermal- (neuronal cells), mesodermal- (skeletal muscle cells), and endodermal- (liver progenitor cells) lineage cells according to tissue microenvironment, and thus PB-SSEA-3(+) cells, tissue-derived Muse cells from the BM, adipose tissue, and umbilical cord behave similarly^{3,5,8,10}.

On the other hand, there are several differences between PB-SSEA-3(+) cells and BM-Muse cells: (1) the mean size of PB-SSEA-3(+) cells ($10.1 \pm 0.3 \mu\text{m}$) is smaller than that of tissue-derived Muse cells ($13 \sim 15 \mu\text{m}$)³; and (2) SSEA-3 is expressed in both PB-SSEA-3(+) cells and BM-Muse cells, while the expression of other markers differs. All of the PB-SSEA-3(+) cells expressed CD45, leukocyte common antigen, while only ~7.5% of freshly isolated BM-Muse cells express CD45. A high proportion of PB-SSEA-3(+) cells expressed CD19 (~85%), a marker for B cells and follicular dendritic cells. BM-Muse cells express CD105, a marker for MSCs that is postulated to be involved in cell adhesion and cytoskeleton arrangement, at a higher proportion (~68%) than PB-SSEA-3(+) cells (~22%). All of human BM-Muse cells were reported to be negative for HLA-DR¹¹, while ~90% of PB-SSEA-3(+) cells were positive for HLA-DR; (3) PB-SSEA-3(+) cells showed 30~90 times higher expression of pluripotency markers than BM-Muse cells; (4) PB-SSEA-3(+) cells did not attach to the culture dish and did not actively proliferate under the conventional culture methods used for tissue-derived Muse cells, including that for BM-Muse cells, although various culture conditions should be evaluated in future studies. Low adherence and low proliferation of PB-SSEA-3(+) cells *in*

vitro is considered pertinent to the microenvironment where PB-Muse cells exist; if PB-SSEA-3(+) cells have high adherence and proliferative activity in the PB, they would easily adhere to vessel walls, potentially inhibiting smooth circulation and causing emboli in vessels. Therefore, these properties seem reasonable for PB-SSEA-3(+) cells.

The marker expression profile of PB-SSEA-3(+) cells, positive for SSEA-3 and CD45, while negative for CD34, CD309 (VEGFR-2), and CD144 (VE-Cadherin), suggests that these cells are distinct from other progenitor/stem cells in the PB. Human hematopoietic stem cells are characterized as CD34+ and Lin⁻²⁵. EPCs are also progenitor/stem cells found in the PB. Premature EPCs are positive for CD34 and CD309 (VEGFR-2), and mature EPCs are positive for CD144 (VE-Cadherin)^{26,27}. MSCs are detectable in the PB^{28,29}, particularly in the presence of mobilizers. MSCs exhibit different properties depending on the tissue origin, however, and the International Society for Cellular Therapy suggested a definition of human MSCs as cells positive for CD73, CD90, and CD105, and negative for CD11b or CD14, CD19 or CD79 α , CD34, CD45, and HLA-DR³⁰. In contrast to MSCs, all of PB-SSEA-3(+) cells were positive for CD45 and ~90% of them were positive for HLA-DR. Very small embryonic-like stem cells have been detected in the mouse BM, human-umbilical cord blood, and human-PB³¹. They are positive for CD34, and negative for CD45 and Lin^{32,33}. Furthermore, very small embryonic-like stem cells are 4~5 μm in mouse and 2~5 μm (after mobilization by granulocyte colony-stimulating factor) or 7~8 μm (in acute myocardial infarction) in humans, and are smaller than PB-SSEA-3(+) cells³²⁻³⁴. Several reports refer to pluripotent-like stem cells found in the PB³⁵⁻³⁷. These reports, however, are based on cultured PB cells, unlike PB-SSEA-3(+) cells, and are CD34(+). Taken together, PB-SSEA-3(+) cells do not appear to be identical to previously reported stem/progenitor cells in the PB.

While SSEA-3 is an established marker for pluripotent stem cells, the SSEA-3 antibody reacts weakly with red blood cells³⁸, which produces a significantly high false positive rate in the PB because the number of red blood cells is considerably higher than the number of rare stem cells. To exclude the possible contamination of red blood cells, we incorporated the Hoechst 33342-staining step in the cell sorting procedure as shown in Fig. 2C and selected the mononuclear cell fraction. We further observed the morphology of PB-SSEA-3(+) cells under laser confocal microscopy and confirmed that they were nucleated cells with a diameter of $10.1 \pm 0.3 \mu\text{m}$, which is larger than that of red blood cells (Fig. 2I).

PB-SSEA-3(+) cells are assumed to be the bone marrow origin because as shown in Fig. 4, SSEA-3(+)/CD45(+) cells are corresponding to ~7.5% of total SSEA-3(+) cells in the BM, and it is plausible that those cells actively mobilized from the BM into the PB. Besides, it is also possible that SSEA-3(+)/CD105(+) cells that occupy 68% of total SSEA-3(+) cells in the BM switch the class from SSEA-

3(+)/CD105(+) to SSEA-3(+)/CD45(+) for mobilization in order to adapt to the microenvironment. Whether or not PB-SSEA-3(+) cells are related to tissue-Muse cells and are a specialized subpopulation of Muse cells, and whether or not PB-SSEA-3(+) cells and tissue-Muse cells constitute different lineages of cells are interesting subjects to be clarified in the future.

Acknowledgments

This study was supported by a Grant-in-Aid for Scientific Research (B) from the Japan Society for the Promotion of Science and Joint Research Funds of Life Science Institute, Inc. Mari Dezawa, Shohei Wakao, and Yoshihiro Kushida of the Department of Stem Cell Biology and Histology, Tohoku University Graduate School of Medicine, are parties to a co-development agreement with Life Science Institute, Inc.

Ethical Approval

This research was approved by the Ethics Review Board according to the guidelines of the Ethics Committee of the Graduate School of Medicine, Tohoku University (Approval Number: 2016-1-516).

Statement of Human and Animal Rights

All animals (male severe-combined immune deficiency [SCID]; CB17/Icr-Prkdc^{scid}/CrjCrlj at 8–10 wk and C57BL/6 mice at 10 wk) were treated in accordance with the Code of Ethics of the World Medical Association and Tohoku University guidelines based on the International Guiding Principles for Biomedical Research Involving Animals. The animal experimental protocol was approved by Tohoku University's Administrative Panel of Laboratory Animal Care (Approval Number: 2016-241). All procedures in this study were conducted in accordance with the Ethics Review Board according to the guidelines of the Ethics Committee of the Graduate School of Medicine, Tohoku University (Approval Number: 2016-1-516) approved protocols.

Statement of Informed Consent

Written informed consent was obtained from each volunteer for their anonymized information to be published in this article.

Declaration of Conflicting Interests

The author(s) declared no potential conflicts of interest with respect to the research, authorship, and/or publication of this article.

Funding

The author(s) disclosed receipt of the following financial support for the research, authorship, and/or publication of this article: This study was supported by collaborative research development with Life Science Institute, Inc., and by Japan society for the promotion of science (JSPS) KAKENHI (Grant Number 16K11393).

ORCID iD

Mari Dezawa  <https://orcid.org/0000-0001-9978-6178>

Supplemental Material

Supplemental material for this article is available online.

References

1. Fisher SA, Zhang H, Doree C, Mathur A, Martin-Rendon E. Stem cell treatment for acute myocardial infarction. *Cochrane Database Syst Rev*. 2015;30(9):CD006536.
2. Zhang Y, Huang B. Peripheral blood stem cells: phenotypic diversity and potential clinical applications. *Stem Cell Rev Rep*. 2012;8(3):917–925.
3. Kuroda Y, Kitada M, Wakao S, Nishikawa K, Tanimura Y, Makinoshima H, Goda M, Akashi H, Inutsuka A, Niwa A, Shigemoto T, et al. Unique multipotent cells in adult human mesenchymal cell populations. *Proc Natl Acad Sci USA*. 2010;107(19):8639–8643.
4. Kuroda Y, Kitada M, Wakao S, Dezawa M. Bone marrow mesenchymal cells: how do they contribute to tissue repair and are they really stem cells? *Arch Immunol Ther Exp (Warsz)*. 2011;59(5):369–378.
5. Heneidi S, Simerman AA, Keller E, Singh P, Li X, Dumesic DA, Chazenbalk G. Awakened by cellular stress: isolation and characterization of a novel population of pluripotent stem cells derived from human adipose tissue. *PLoS One*. 2013;8(6):e64752.
6. Gimeno ML, Fuertes F, Barcala Tabarozzi AE, Attorressi AI, Cucchiani R, Corrales L, Oliveira TC, Sogayar MC, Labriola L, Dewey RA, Perone MJ. Pluripotent nontumorigenic adipose tissue-derived muse cells have immunomodulatory capacity mediated by transforming growth factor-beta1. *Stem Cells Transl Med*. 2017;6(1):161–173.
7. Alessio N, Ozcan S, Tatsumi K, Murat A, Peluso G, Dezawa M, Galderisi U. The secretome of MUSE cells contains factors that may play a role in regulation of stemness, apoptosis and immunomodulation. *Cell Cycle*. 2017;16(1):33–44.
8. Ogura F, Wakao S, Kuroda Y, Tsuchiyama K, Bagheri M, Heneidi S, Chazenbalk G, Aiba S, Dezawa M. Human adipose tissue possesses a unique population of pluripotent stem cells with nontumorigenic and low telomerase activities: potential implications in regenerative medicine. *Stem Cells Dev*. 2014;23(7):717–728.
9. Amin M, Kushida Y, Wakao S, Kitada M, Tatsumi K, Dezawa M. Cardiogenic growth factor-driven induction of human muse cells into cardiomyocyte-like phenotype. *Cell Transplant*. 2018;27(2):285–298.
10. Korecka JA, Talbot S, Osborn TM, de Leeuw SM, Levy SA, Ferrari EJ, Moskites A, Atkinson E, Jodelka FM, Hinrich AJ, Hastings ML, et al. Neurite collapse and altered ER Ca(2+) control in human parkinson disease patient ipsc-derived neurons with LRRK2 G2019 S mutation. *Stem Cell Reports*. 2019;12(1):29–41.
11. Tanaka T, Nishigaki K, Minatoguchi S, Nawa T, Yamada Y, Kanamori H, Mikami A, Ushikoshi H, Kawasaki M, Dezawa M, Minatoguchi S. Mobilized muse cells after acute myocardial infarction predict cardiac function and remodeling in the chronic phase. *Circ J*. 2018;82(2):561–571.
12. Uchida H, Morita T, Niizuma K, Kushida Y, Kuroda Y, Wakao S, Sakata H, Matsuzaka Y, Mushiaki H, Tominaga T, Borlongan CV, et al. Transplantation of unique subpopulation of

- fibroblasts, muse cells, ameliorates experimental stroke possibly via robust neuronal differentiation. *Stem Cells*. 2016;34(1):160–173.
13. Uchida H, Niizuma K, Kushida Y, Wakao S, Tominaga T, Borlongan CV, Dezawa M. Human muse cells reconstruct neuronal circuitry in subacute lacunar stroke model. *Stroke*. 2017;48(2):428–435.
 14. Iseki M, Kushida Y, Wakao S, Akimoto T, Mizuma M, Motoi F, Asada R, Shimizu S, Unno M, Chazenbalk G, Dezawa M. Muse cells, nontumorigenic pluripotent-like stem cells, have liver regeneration capacity through specific homing and cell replacement in a mouse model of liver fibrosis. *Cell Transplant*. 2017;26(5):821–840.
 15. Ozuru R, Wakao S, Tsuji T, Ohara N, Matsuba T, Amuran MY, Isobe J, Iino M, Nishida N, Matsumoto S, Iwadate K, et al. Rescue from Stx2-producing *e. coli*-associated encephalopathy by intravenous injection of muse cells in NOD-SCID mice. *Mol Ther*. 2020;28(1):100–118.
 16. Hori E, Hayakawa Y, Hayashi T, Hori S, Okamoto S, Shibata T, Kubo M, Horie Y, Sasahara M, Kuroda S. Mobilization of pluripotent multilineage-differentiating stress-enduring cells in ischemic stroke. *J Stroke Cerebrovasc Dis*. 2016;25(6):1473–1481.
 17. Livak KJ, Schmittgen TD. Analysis of relative gene expression data using real-time quantitative PCR and the 2(-Delta Delta C(T)) Method. *Methods*. 2001;25(4):402–408.
 18. Pijuan-Galito S, Tamm C, Schuster J, Sobol M, Forsberg L, Merry CL, Anneren C. Human serum-derived protein removes the need for coating in defined human pluripotent stem cell culture. *Nat Commun*. 2016;13(7):12170.
 19. Petrie RJ, Doyle AD, Yamada KM. Random versus directionally persistent cell migration. *Nat Rev Mol Cell Biol*. 2009;10(8):538–549.
 20. Rosen H, Goetzl EJ. Sphingosine 1-phosphate and its receptors: an autocrine and paracrine network. *Nat Rev Immunol*. 2005;5(7):560–570.
 21. Blaho VA, Hla T. Regulation of mammalian physiology, development, and disease by the sphingosine 1-phosphate and lysophosphatidic acid receptors. *Chem Rev*. 2011;111(10):6299–6320.
 22. Cyster JG, Schwab SR. Sphingosine-1-phosphate and lymphocyte egress from lymphoid organs. *Annu Rev Immunol*. 2012;30:69–94. doi:10.1146/annurev-immunol-020711-075011.
 23. Abe T, Aburakawa D, Niizuma K, Iwabuchi N, Kajitani T, Wakao S, Kushida Y, Dezawa M, Borlongan CV, Tominaga T. Intravenously transplanted human Muse cells afford brain repair in a mouse lacunar stroke model. *Stroke*. 2020;51(2):601–611. in press.
 24. Katagiri H, Kushida Y, Nojima M, Kuroda Y, Wakao S, Ishida K, Endo F, Kume K, Takahara T, Nitta H, Tsuda H, et al. A distinct subpopulation of bone marrow mesenchymal stem cells, muse cells, directly commit to the replacement of liver components. *Am J Transplant*. 2016;16(2):468–483.
 25. Srour EF, Brandt JE, Briddell RA, Leemhuis T, van Besien K, Hoffman R. Human CD34+ HLA-DR- bone marrow cells contain progenitor cells capable of self-renewal, multilineage differentiation, and long-term *in vitro* hematopoiesis. *Blood Cells*. 1991;17(2):287–295.
 26. Asahara T, Murohara T, Sullivan A, Silver M, van der Zee R, Li T, Witzenbichler B, Schatteman G, Isner JM. Isolation of putative progenitor endothelial cells for angiogenesis. *Science*. 1997;275(5302):964–967.
 27. Hristov M, Erl W, Linder S, Weber PC. Apoptotic bodies from endothelial cells enhance the number and initiate the differentiation of human endothelial progenitor cells *in vitro*. *Blood*. 2004;104(9):2761–2766.
 28. Wexler SA, Donaldson C, Denning-Kendall P, Rice C, Bradley B, Hows JM. Adult bone marrow is a rich source of human mesenchymal ‘stem’ cells but umbilical cord and mobilized adult blood are not. *Br J Haematol*. 2003;121(2):368–374.
 29. Zvaifler NJ, Marinova-Mutafchieva L, Adams G, Edwards CJ, Moss J, Burger JA, Maini RN. Mesenchymal precursor cells in the blood of normal individuals. *Arthritis Res*. 2000;2(6):477–488.
 30. Dominici M, Le Blanc K, Mueller I, Slaper-Cortenbach I, Marini F, Krause D, Deans R, Keating A, Prockop D, Horwitz E. Minimal criteria for defining multipotent mesenchymal stromal cells. The International Society for Cellular Therapy position statement. *Cytotherapy*. 2006;8(4):315–317.
 31. Kucia M, Reza R, Campbell FR, Zuba-Surma E, Majka M, Ratajczak J, Ratajczak MZ. A population of very small embryonic-like (VSEL) CXCR4(+)/SSEA-1(+)/Oct-4+ stem cells identified in adult bone marrow. *Leukemia*. 2006;20(5):857–869.
 32. Kucia MJ, Wysoczynski M, Wu W, Zuba-Surma EK, Ratajczak J, Ratajczak MZ. Evidence that very small embryonic-like stem cells are mobilized into peripheral blood. *Stem Cells*. 2008;26(8):2083–2092.
 33. Wojakowski W, Tendera M, Kucia M, Zuba-Surma E, Paczkowska E, Ciosek J, Halasa M, Krol M, Kazmierski M, Buszman P, Ochala A, et al. Mobilization of bone marrow-derived Oct-4+ SSEA-4+ very small embryonic-like stem cells in patients with acute myocardial infarction. *J Am Coll Cardiol*. 2009;53(1):1–9.
 34. Sovalat H, Scrofani M, Eidenschenk A, Pasquet S, Rimelen V, Henon P. Identification and isolation from either adult human bone marrow or G-CSF-mobilized peripheral blood of CD34(+)/CD133(+)/CXCR4(+)/Lin(-)CD45(-) cells, featuring morphological, molecular, and phenotypic characteristics of very small embryonic-like (VSEL) stem cells. *Exp Hematol*. 2011;39(4):495–505.
 35. Zhao Y, Glesne D, Huberman E. A human peripheral blood monocyte-derived subset acts as pluripotent stem cells. *Proc Natl Acad Sci USA*. 2003;100(5):2426–2431.
 36. Kuwana M, Okazaki Y, Kodama H, Izumi K, Yasuoka H, Ogawa Y, Kawakami Y, Ikeda Y. Human circulating CD14+ monocytes as a source of progenitors that exhibit mesenchymal cell differentiation. *J Leukoc Biol*. 2003;74(5):833–845.

37. Freyman T, Polin G, Osman H, Crary J, Lu M, Cheng L, Palasis M, Wilensky RL. A quantitative, randomized study evaluating three methods of mesenchymal stem cell delivery following myocardial infarction. *Eur Heart J.* 2006;27(9): 1114–1122.
38. Kannagi R, Cochran NA, Ishigami F, Hakomori S, Andrews PW, Knowles BB, Solter D. Stage-specific embryonic antigens (SSEA-3 and -4) are epitopes of a unique globo-series ganglioside isolated from human teratocarcinoma cells. *EMBO J.* 1983;2(12):2355–2361.